

Fronts  
Tidal mixing  
Stratification

Fronts  
Mélange dû à la marée  
Stratification

# The structure and variability of shelf sea fronts as observed by an undulating CTD system

C. M. Allen<sup>a,c</sup>, J. H. Simpson<sup>a</sup>, R. M. Carson<sup>b,d</sup>

<sup>a</sup>Department of Physical Oceanography, Marine Science Laboratories, Menai Bridge, Anglesey, GB.

<sup>b</sup>Institute of Oceanographic Sciences, Brook Road, Wormley, Surrey, GB.

<sup>c</sup>Present address: Department of Applied Mathematics and Theoretical Physics, University of Liverpool, P.O. Box 147, Liverpool L69 3BX, GB.

<sup>d</sup>Present address: Department of Mechanical Engineering, University of Nairobi, P.O. Box 30197, Nairobi, Kenya.

Received 20/4/79, in revised form 11/9/79, accepted 14/9/79.

## ABSTRACT

Detailed observations of the structure of shelf sea fronts have been made by means of an undulating towed CTD. The high resolution data reveal a complex pattern of variability in both space and time; seasonal development and the effects of wind stirring on the frontal structure are also illustrated. An estimate of the variation in the efficiency of tidal mixing,  $e$ , on the basis of the observed potential energy,  $(\bar{V})$ , distribution is suggestive of a positive feedback process in the establishment of stratification. Such a process would be consistent with recent observations which show that the fronts do not adjust significantly during the spring-neaps cycle as predicted by the vertical mixing model of James (1977).

*Oceanol. Acta*, 1980, 3, 1, 59-68.

## RÉSUMÉ

Variabilité de fronts marins sur le plateau continental.  
Observations à l'aide d'une sonde CTD  
à trajectoire verticale sinusoïdale

Nous avons fait des observations détaillées de la structure des fronts de mer sur le plateau continental à l'aide d'une sonde CTD remorquée sur une trace d'allure sinusoïdale. Les données de haute résolution obtenues rendent compte d'une configuration compliquée de la variabilité à la fois dans le domaine spatial et le domaine temporel. L'apparition saisonnière de la structure frontale avec les effets de l'agitation due au vent apparaissent. Une évaluation de l'importance plus ou moins grande du mélange entraîné par la marée suggère, sur la base d'observations de l'énergie potentielle  $(\bar{V})$ , un processus de feed-back positif pour l'établissement de la stratification. Un tel mécanisme serait en accord avec des observations récentes qui montrent que les fronts ne se modifient guère au cours du cycle de variation de la marée entre vives eaux et mortes eaux, ainsi qu'avait prévu le modèle de mélange vertical de James (1977).

*Oceanol. Acta*, 1980, 3, 1, 59-68.

## INTRODUCTION

A shallow sea front represents the boundary between stratified and vertically mixed water columns, and is

characterised by sharp horizontal gradients in physical, chemical and biological parameters.

Investigations have shown such regions to occur, for example, in the western Irish Sea, to the south-west of

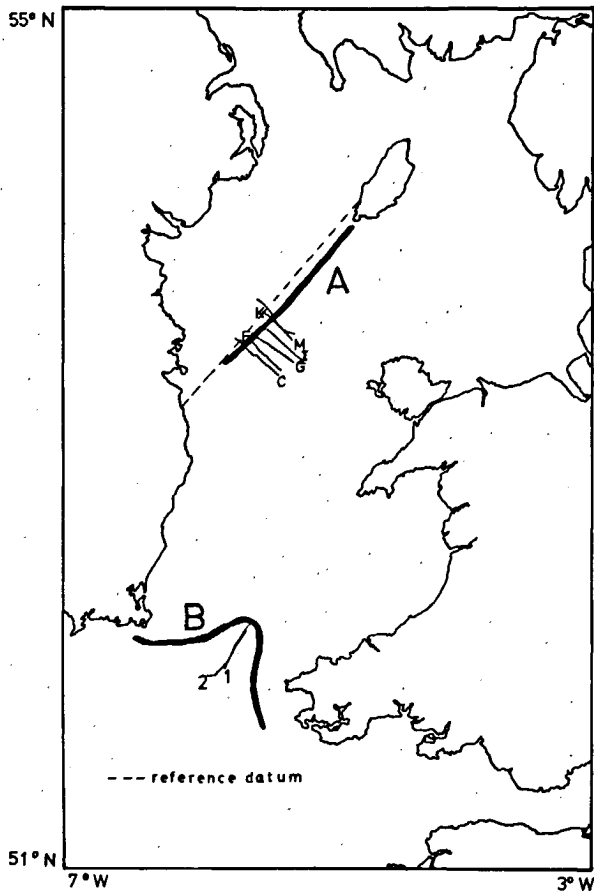


Figure 1  
Heavy lines represent the mean positions of the fronts taken from a composite of satellite infra-red images.  
A: western Irish Sea front; B: Celtic sea front. Solid lines designate sections discussed in this paper.

the Isle of Man, and in St. Georges Channel (Fig. 1). Surveys by Simpson (1976), taking vertical STD profiles across a front, and by Bruce and Aiken (1975), using an undulating towed recorder, have outlined the basic structure of these fronts. They occur in the summer months and are controlled by a balance between a seasonally varying heat flux input and variations in the level of tidal mixing in the area (Simpson, Hunter, 1974).

If we extend this model to include the effect of wind mixing, the overall potential energy balance may be written (Simpson, Allen, Morris, 1978):

$$\frac{dV}{dt} = -\frac{\alpha g \dot{Q} h}{2c} + \epsilon k_b \rho \bar{u}_b^3 + \delta k_s \rho_s \bar{W}^3 \quad (1)$$

if the potential energy relative to a mixed state is

$$V = \bar{V}h = \int_{-h}^0 (\rho - \bar{\rho})gzdz; \quad \bar{\rho} = \frac{1}{h} \int_{-h}^0 \rho dz,$$

where  $\rho$  is density and  $h$  the depth of the water column. The first term in equation (1) represents the surface heating term where:

$\alpha$  = volume expansion coefficient;

$\dot{Q}$  = rate of heat input;

$c$  = specific heat.

The second and third terms are the tidal and wind mixing terms respectively where:

$\epsilon$  and  $\delta$  are the efficiencies of tide and wind mixing;

$\rho$  and  $\rho_s$  are water and air densities;

$k_b$  and  $k_s$  are drag coefficients;

$u_b$  = near bottom velocity;

$W$  = windspeed near the sea surface.

For a vertically mixed region  $V=0$  and for increasingly stable stratification  $V$  becomes negative. When  $V < 0$  tidal and wind mixing thus bring about positive changes in  $V$ , whereas surface heating results in an increasingly negative  $V$ .

Frontogenesis begins in April or May when there is an increase in the solar heat input to the sea surface, and increases to a maximum by July when there may be a vertical temperature difference of 7°C in a 50 m depth interval, and a horizontal surface temperature gradient of ~1°C per kilometre. The decrease in the heat flux input and the onset of winter storms act to break down the thermocline, and by November the region is usually well mixed again.

The horizontal density gradients set up pressure forces which cause accelerations resulting in a velocity field in which pressure gradients and frictional forces are balanced by the geostrophic accelerations. James (1978) has calculated the flow induced by a shallow sea front using a two-dimensional numerical model. He assumes that the front can be represented by a fixed density structure maintained by a balance of heating, evaporation, horizontal and vertical mixing and advection, and examines the currents which would be driven by the resulting horizontal density gradients. The model shows a significant circulation in the vertical plane with upwelling on the well mixed side of the front; there is a weaker circulation on the stratified side of the front which is in the opposite sense to that on the well mixed side. This produces a strong convergence which is reported in connection with these fronts (Simpson, Allen, Morris, 1978). This convergence is one of the factors possibly responsible for anomalies in biomass and nutrient distributions which have recently been observed in frontal regions (Savidge, 1976; Pingree, Holligan, Head, 1977).

In this paper we present the results of observations made with an undulating, towed CTD in both the western Irish Sea and Celtic Sea frontal regions. After the application of detailed tidal corrections and calibrations, the data is examined to ascertain the degree of spatial variability and time dependence in these features.

## UNDULATING CTD SYSTEM

The suspected variability of the frontal system both in space and time calls for the rapid execution of high resolution profiles. This suggests the use of the Batfish as a primary tool for frontal studies. The Batfish (Dessureault, 1976), is a cable towed body which can

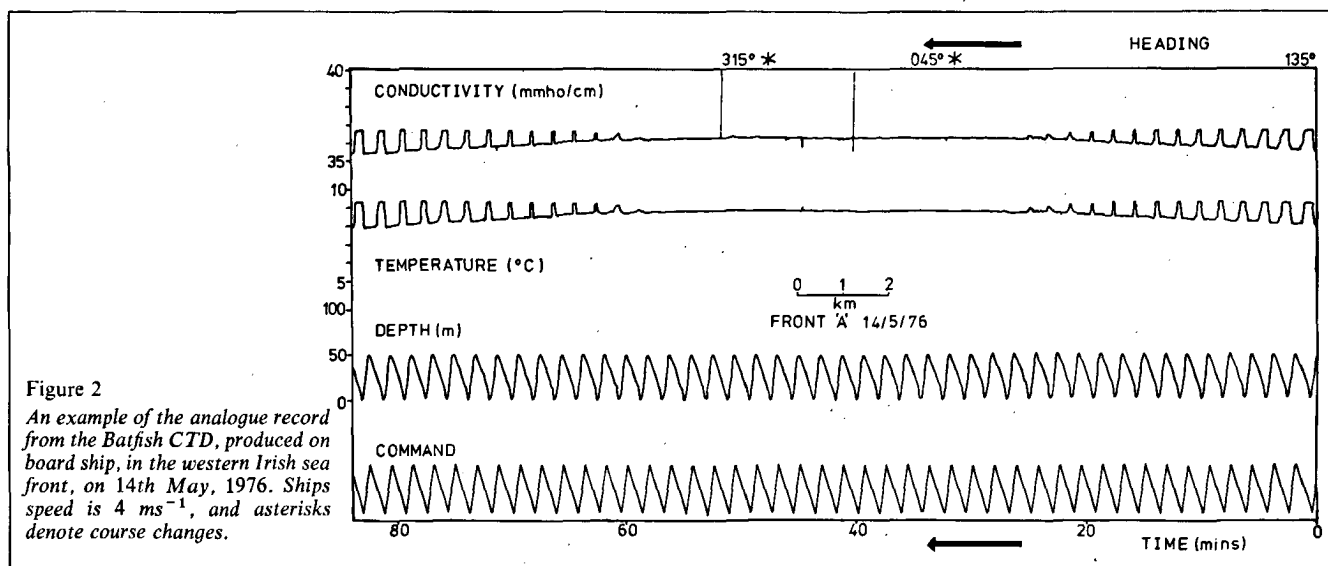


Figure 2

An example of the analogue record from the Batfish CTD, produced on board ship, in the western Irish sea front, on 14th May, 1976. Ships speed is  $4 \text{ ms}^{-1}$ , and asterisks denote course changes.

undulate in depth on command from the ship. Our instrument is the wide wing version; it was towed at  $3\text{--}4 \text{ ms}^{-1}$  on  $\sim 80 \text{ m}$  of unfaired cable, and typically undulated from near-surface to  $50 \text{ m}$  depth, with an undulation period of  $100\text{--}120$  seconds. The water depth was  $\sim 100 \text{ m}$  in both the western Irish Sea and the Celtic Sea areas and the thermocline depth was  $20\text{--}40 \text{ m}$ , so the profile extended to the colder mixed water below the thermocline. The horizontal sampling produced by the Batfish is governed by the speed of the ship, and the rates of ascent and descent of the Batfish.

The maximum distance between surface data points  $d$ , is given by:

$$d = 2h^1 u^1 / w \text{ (m);}$$

where

$u^1$  = speed of ship ( $\text{ms}^{-1}$ );

$h^1$  = maximum depth of Batfish descent (m);

$w$  = average vertical velocity ( $\text{ms}^{-1}$ );

The mid-depth spacing will be  $d/2$ . Typical maximum values of  $u^1 \sim 4 \text{ ms}^{-1}$ ,  $w \sim 1 \text{ ms}^{-1}$  and  $h^1 \sim 50 \text{ m}$  give  $d \sim 400 \text{ m}$ .

The Batfish used in these observations has been modified to increase the reliability of the hydraulic servo system which has now been rebuilt and enclosed in an oil filled outer case, with double seals, to prevent the ingress of seawater to the hydraulic unit. Recently the body has also been altered to increase the instrument space and to provide a convenient chassis for mounting alternative instruments.

The CTD employed in the Batfish is a Neil Brown type (Brown, 1974), which samples at  $32 \text{ Hz}$ . The response time of the temperature and conductivity sensors is  $0.025$  second and with maximum horizontal and vertical velocities of  $4$  and  $1 \text{ ms}^{-1}$  the sample spacing is  $400/32$  ( $12.5 \text{ cm}$ ) and  $100/32$  ( $3.125 \text{ cm}$ ) respectively.

The stability of both temperature and conductivity measurements is particularly important for Batfish work, as the instrument may be towed for  $12\text{--}24$  hours without a break and calibration points are only obtained (by

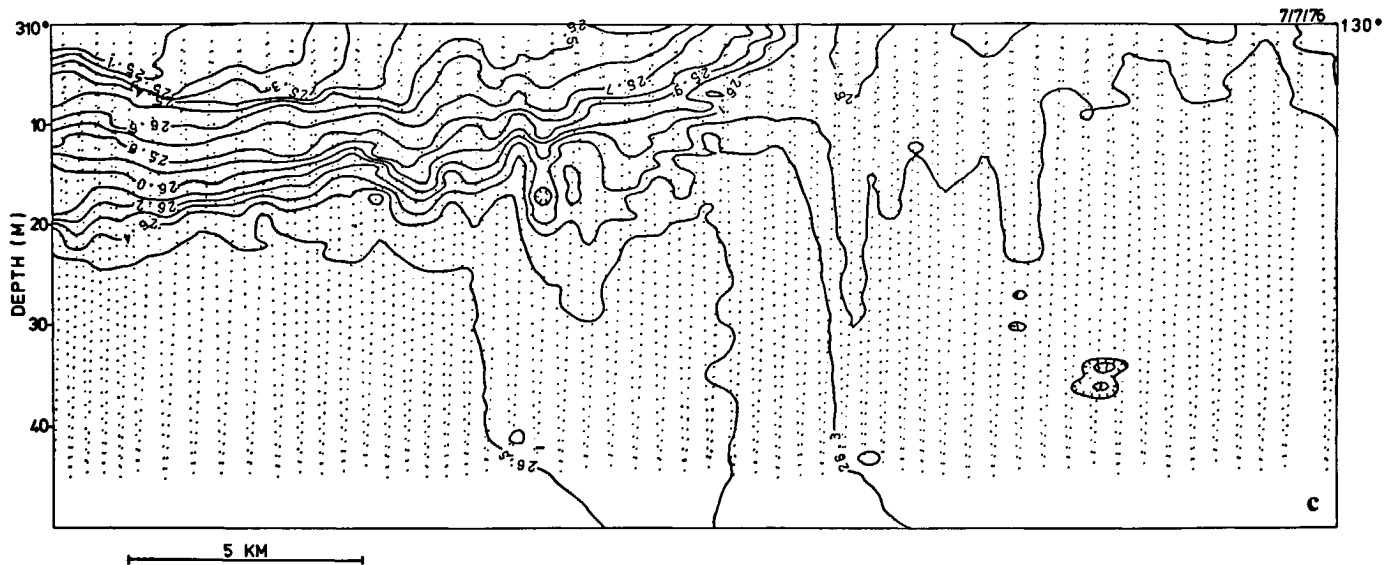
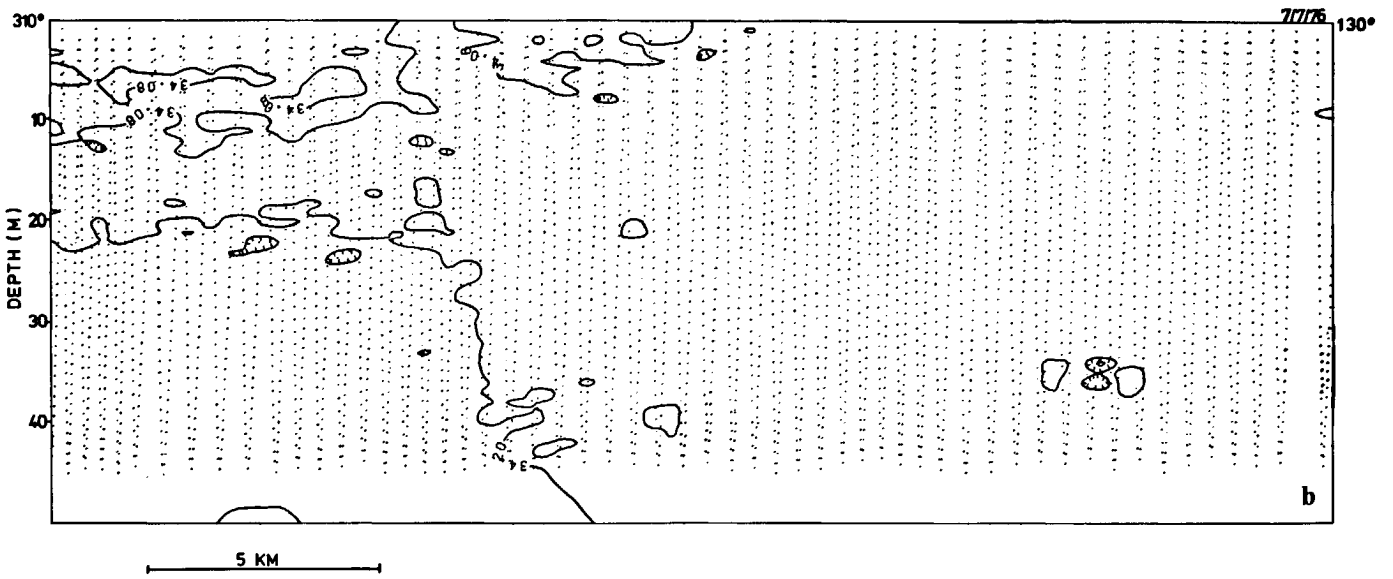
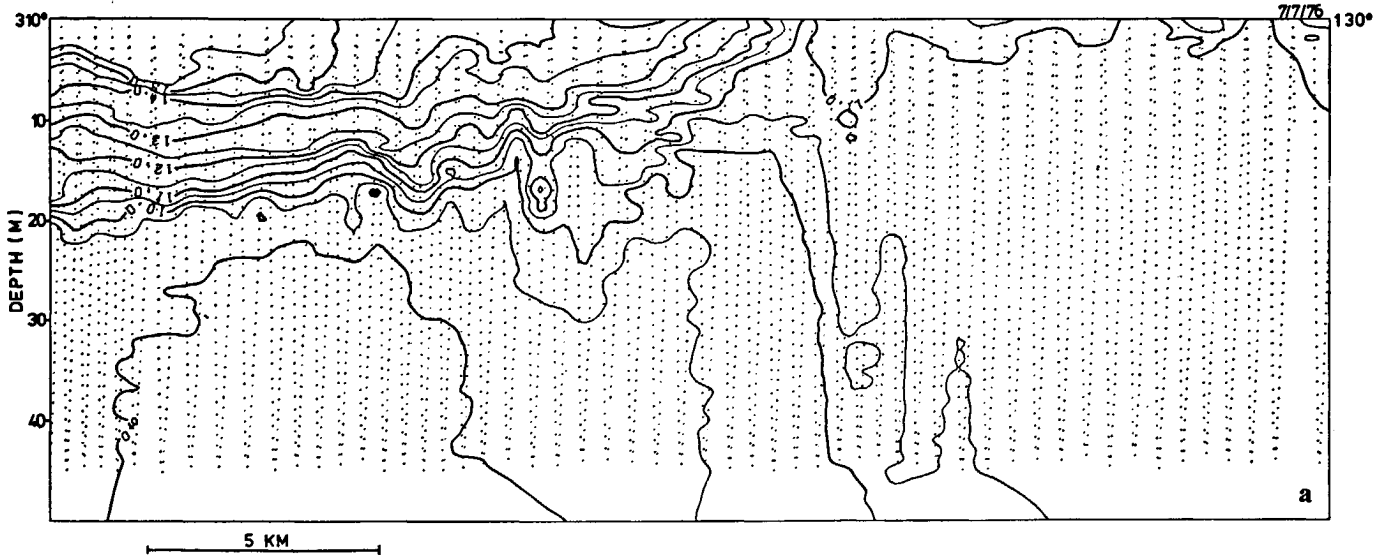
comparison with an NIO water bottle and reversing thermometer) at the beginning and end of each run. The recent development of a four-bottle multisampler, operated from the ship on command, will improve matters. The conductivity cell is liable to fouling, particularly by siphonophores, and these cause occasional jumps in the conductivity records. Usually the cell clears itself within a few seconds and returns to its previous level; such jumps have been removed from the records in the subsequent processing. In the event of serious permanent fouling the instrument must be recovered and cleaned.

The CTD FM signal is converted to an analogue voltage and displayed on a multichannel pen recorder; this allows one to see the degree of stratification and the position of the front, and enables the ship time to be used to maximum advantage. An example of an analogue record taken during a cruise in the western Irish Sea region, at the onset of stratification in May 1976, is shown in Figure 2. The Batfish depth trace follows the command signal very closely. The maximum vertical temperature difference is slightly less than  $1.5^\circ\text{C}$  and this decreases towards the mixed region where there is virtually no variation in temperature.

## DATA PROCESSING

The FM signal is also recorded on audio tape which is subsequently reformatted, via a Hewlett-Packard 2100 A mini computer, to produce computer compatible digital magnetic tape. This tape contains pressure, temperature and conductivity values recorded at  $32 \text{ ms}$  intervals.

A typical section across a front, of  $2$  hours duration at a speed of  $\sim 4 \text{ ms}^{-1}$ , would produce a data set containing  $\sim 2.3 \times 10^5$  values each of pressure, temperature and conductivity. Once spurious points are eliminated from the data set, it is calibrated and then decimated according to a specified input pressure difference to yield a time series of pressure, temperature, conductivity, salinity and  $\sigma\text{-}t$  (density) values.



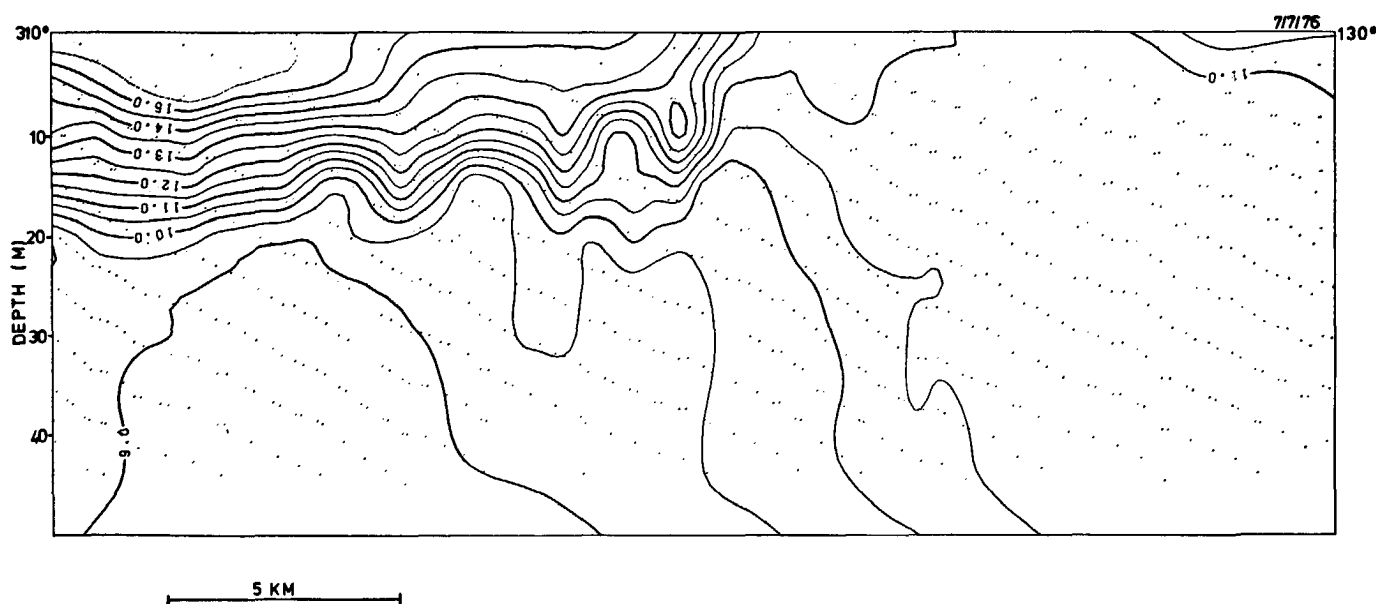


Figure 4

Temperature field on the same vertical section as Figure 3. The dots represent data points used in the contour analysis. Vertical data spacing is 5 m. Contour interval is 0.5°C.

The position of the frontal interface changes throughout the tidal cycle and we assume, to a first approximation, that it is advected as a frozen field. The ship's position is corrected for the tidal displacement, using tidal streams data from a numerical model of the Irish Sea (Hunter, personal communication), and the time series of CTD data is fitted to this tidally corrected track. Contouring of this data gives the temperature, density and salinity fields on vertical sections across the front. The large amounts of data produced by the Batfish surveys require that the contour program should accept up to seven or eight thousand points for one map, thus using the high resolution data to its best advantage. The package used is the Calcomp-General Purpose Contouring Package; it takes the irregularly spaced temperature, salinity and sigma- $t$  values (up to nine thousand points per map) and interpolates to produce data on a user-defined rectangular grid, from which contours are generated. This program gives the user considerable control over both the grid point interpolation and the contours plotted. The number of nearest neighbour points used to calculate the surface height and gradient for a particular grid point can be specified and, for example, the regular data array printed out to use in calculations of the

potential energy and heat content of a vertical water column.

An example of the temperature, salinity and density (sigma- $t$ ) fields across the western Irish Sea front in July 1976, using the Batfish CTD data is shown in Figure 3. With the highest horizontal resolution (0.5 km) and a vertical sampling interval of 1 m, the complexity of the frontal region is clearly illustrated. The density structure (Fig. 3 c) is predominantly controlled by temperature (Fig. 3 a); with salinity (Fig. 3 b) playing only a minor role. A typical temperature difference,  $\Delta T \sim 6.5^\circ\text{C}$  produces  $(\Delta\sigma_T)_S \sim 1.6$  and a typical  $\Delta S \sim 0.1$  ppt produces  $(\Delta\sigma_T)_T \sim 0.1$ . The isotherm structure is convoluted (Fig. 3 a) with temperature inversions occurring on scales of  $\sim 0.5$  km horizontal and 2-3 m vertical.

The sections shown in Figure 3 are not inconsistent with those found in previous studies with conventional CTDS, but the wealth of horizontal structure would have been aliased by the larger horizontal sampling interval. The effect produced by varying the vertical spacing is illustrated by comparing Figures 3 a and 4; inversions, manifest at high resolution are much less pronounced in the data with 5 m vertical spacing. The sections using this vertical interval provide a first-look at the CTD data, giving an assessment of the quality of the data and an overall picture of the frontal structure.

#### Figure 3

Vertical sections (orientation 310-130°) across the western Irish sea front on 7th July, 1976 (G in Figure 1). The dots represent data points used in the contour analysis. Vertical data spacing is 1 m. The tidal streams data used for the tidal corrections were obtained from a numerical model of the Irish Sea (Hunter, personal communication).  
Wind: NW  $6 \text{ ms}^{-1}$ .  
Tide: Neaps +2 days. Ebb.

(a) Temperature. Contour interval is 0.5°C.

(b) Salinity. Contour interval is 0.12 ppt.

(c) Sigma- $t$  (density). Contour interval is 0.1 units of  $\sigma_t$ .

## RESULTS

### Seasonal development

The seasonal development of the western Irish sea front between May and July is illustrated in Figures 5 and 6.

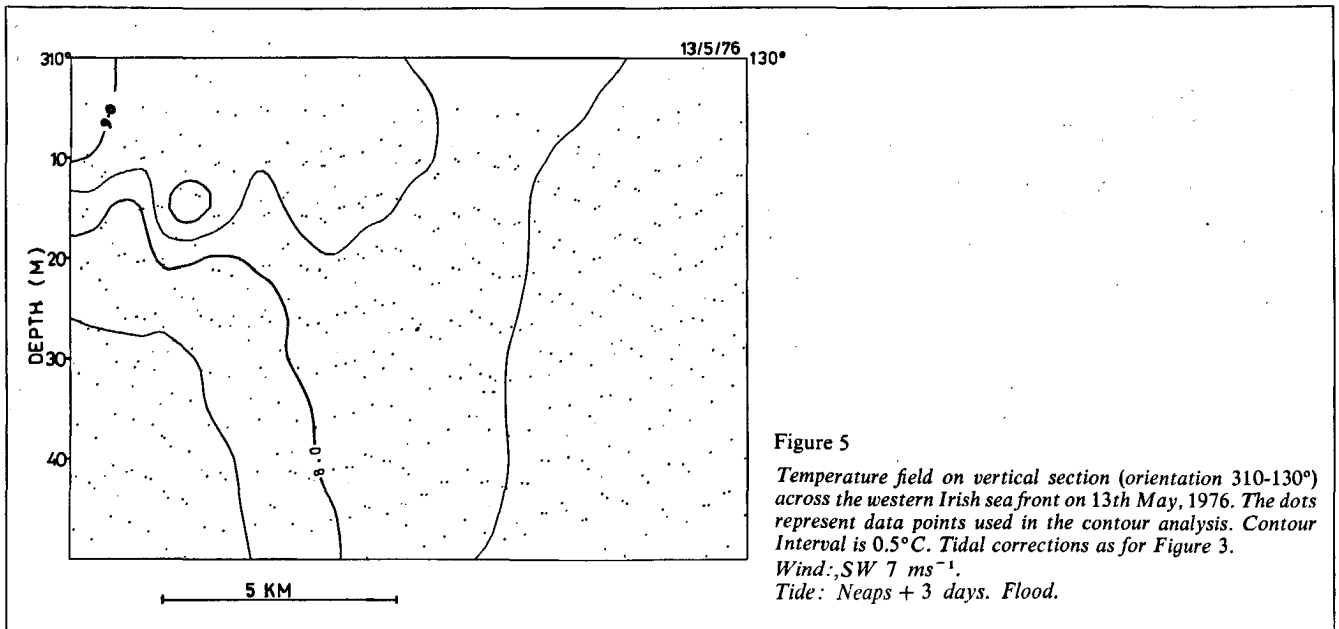


Figure 5  
 Temperature field on vertical section (orientation 310-130°) across the western Irish sea front on 13th May, 1976. The dots represent data points used in the contour analysis. Contour Interval is 0.5°C. Tidal corrections as for Figure 3.  
 Wind: SW 7 ms<sup>-1</sup>.  
 Tide: Neaps + 3 days. Flood.

Figure 5 shows the temperature field just after the onset of stratification in May. In the stratified region, there is a surface mixed layer of ~ 20 m, with the pycnocline occurring between 20 and 40 m depth. The vertical temperature difference in the stratified water is 1.5°C and the temperature of the mixed region is constant to within 0.01°C. The horizontal surface temperature gradient is ~ 0.2°C per kilometre.

By July (Fig. 6), the vertical temperature difference on the same section has increased to 7°C and the horizontal surface temperature gradient is almost 2°C per kilometre; the outcrop of the front at the surface is much more intense. There is a suggestion of upwelling occurring close to the front on the well mixed side. This upward displacement of the isotherms extends to the surface where there is an associated minimum in the sea surface temperature.

Between May and July, the potential energy of a water column in the stratified region,  $\bar{V}$ , decreases from ~ -10 to ~ -70 J.m<sup>-3</sup>. These changes are not inconsistent with deductions from historical data (Simpson, Hughes, Morris, 1977).

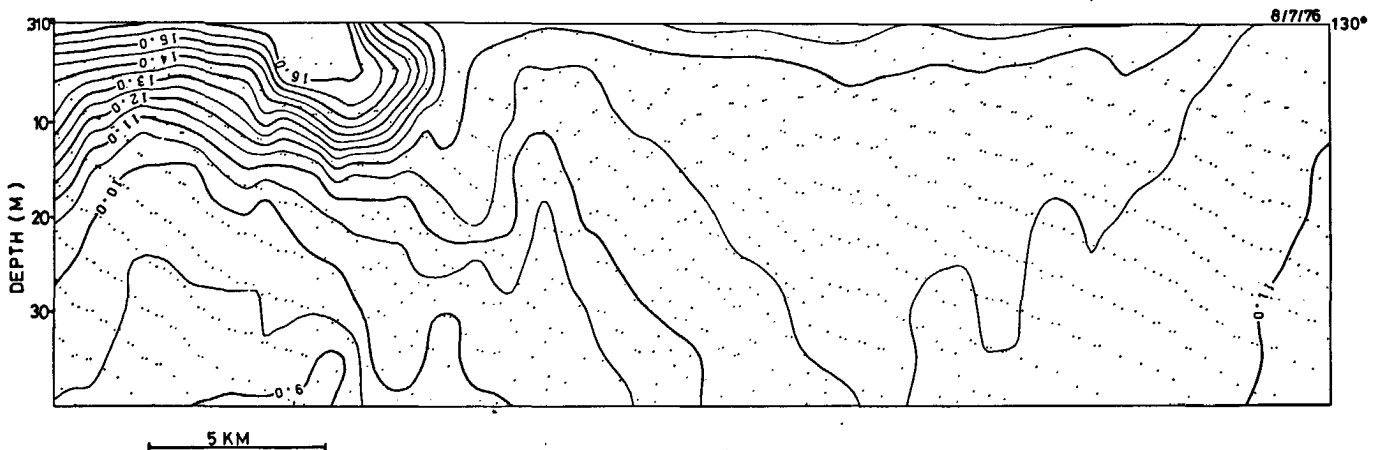
**Changes in structure during a tidal cycle**

The time variability of the frontal structure was investigated by repeated crossings of one particular section across the western Irish Sea front (K in Figure 1) during a single tidal cycle (12 1/2 hours) and is illustrated in Figure 7.

The major axis of the almost degenerate tidal ellipse varies between N-S at the southern end of the front to

Figure 6  
 Temperature field on vertical section (orientation 310-130°) across western Irish sea front on 8th July, 1976 (marked M in Figure 1) The dots represent data points used in the contour analysis. Contour interval is

0.5°C. Tidal corrections as in Figure 3.  
 Wind: N 1 ms<sup>-1</sup>.  
 Tide: Neaps + 3 days. Flood.



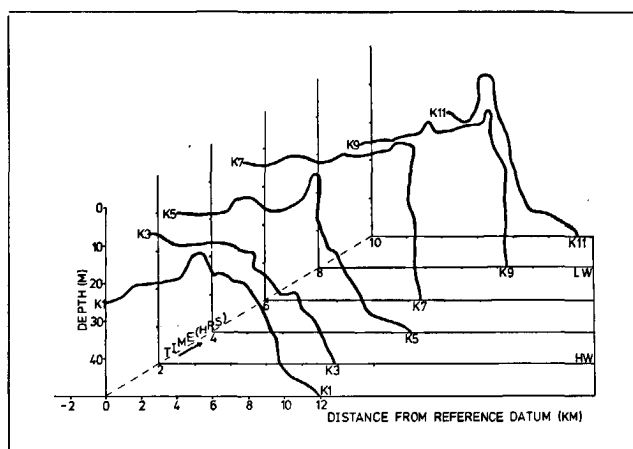


Figure 7  
Variation of 11°C isotherm throughout one tidal cycle (121/2 hrs.) across section K (marked in Figure 1) on 6th July 1976. The sections are adjusted with respect to the reference datum in Figure 1. State of tide: Neaps.

NNE-SSW at the northern end (Hunter, personal communication); the component of surface tidal velocity along the plane of the Batfish sections ( $130\text{--}310^\circ$ ) varied from  $0\text{--}0.25\text{ ms}^{-1}$  (tidal stream excursion 4 km) compared with the total tidal stream excursion of  $\sim 10$  km.

The mean isotherm slope varied significantly during the tidal cycle achieving maximum steepness around low water. The tidal shear was estimated from the horizontal displacements of the isotherms at different depths, throughout the tidal cycle. Between 20 and 45 m, the mean shear is  $\sim 0.4 \times 10^{-3}\text{ sec}^{-1}$  which is significantly larger ( $\times 6$ ) than indicated by empirical formulae for the homogeneous density case (Bowden, Fairbairn, 1952). This apparently implies that a substantial fraction of the vertical shear is concentrated in the pycnocline. However this interpretation does not allow for the effects of the considerable tidal advection parallel to the front which will also contribute to the observed straining.

### Spatial variability

An estimate of true spatial variability along a front

Figure 8  
Variation of 10°C surface along the front in the western Irish sea. The oblique projection shows a three-dimensional view of front. The dotted line is the reference datum drawn in Figure 1; the sections are all tidally corrected and their relative positions are adjusted with respect to this datum (sections marked in Figure 1).

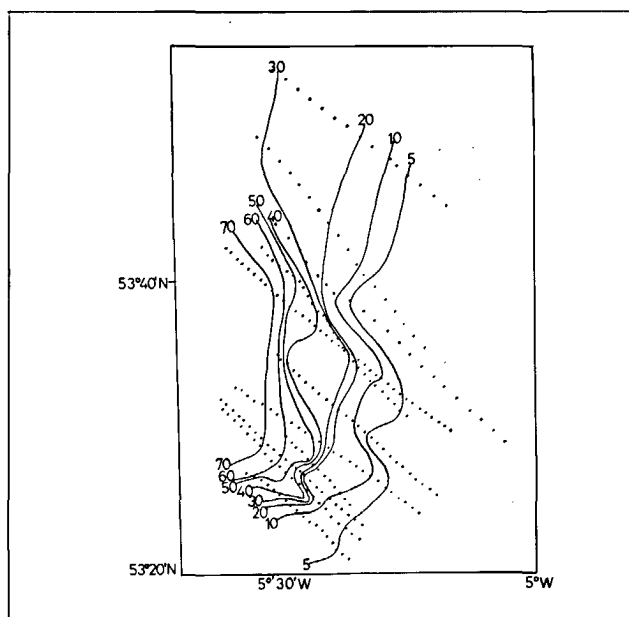
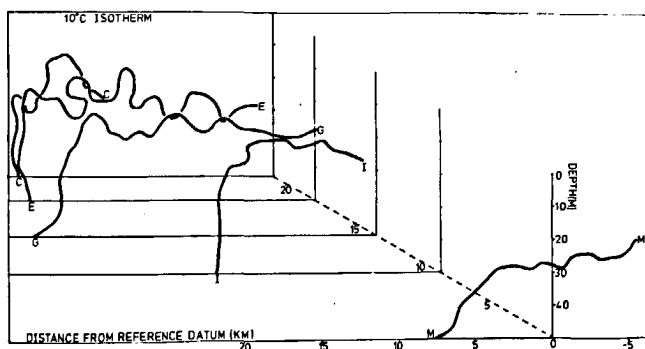


Figure 9  
Contours of  $\bar{V}$  (potential energy of a water column) in the western Irish sea. The dotted line represents sections along which Batfish CTD data was collected, and used for the computations.

requires a synoptic picture of the frontal region. The technique of sampling, using the Batfish CTD, approaches this objective more closely than any previous method of vertical profiling. The survey strategy in the western Irish Sea frontal region was designed to minimise the ambiguity between spatial and temporal variability. The ship's heading was kept steady at  $130^\circ$  or  $310^\circ$  with  $\sim 2\text{--}3$  km spacing between sections (denoted by C, G, E, I, M in Figure 1) during a 32 hour survey.

Figure 8 demonstrates the along-front variability in the western Irish Sea by means of an oblique projection, which illustrates the variations in pattern and differing degree of convolution of the 10°C isotherm. Analysis of the whole temperature field shows an increase in the amplitude of these convolutions as they approach the front. They are probably internal waves, of amplitude  $\sim 4$  m and wavelength  $\sim 3$  km, which begin to break at the frontal interface.

Some of the observed variability in the isotherm structure arises from the tidal straining already discussed, but additional variability is apparent when each section in Figure 8 is compared with the relevant section for the particular state of tide in Figure 7, e. g. section G is not as steep as section K 9 for the same state of tide.

An alternative representation of spatial variability may be obtained by contouring  $\bar{V}$  (mean potential energy density of a water column) and thereby including both temperature and salinity effects (Fig. 9). The potential energy of each column is calculated using the Batfish CTD data. The order of the  $\bar{V}$  contours is in contrast to the complexity of the vertical density sections. The gradient of  $\bar{V}$  normal to the front varies between 3 and  $7\text{ J.m}^{-3}.\text{km}^{-1}$ . This is consistent with values measured in the Islay front (Simpson, Edelsten, Edwards, Morris, Tett, 1978), although that front is affected to a large extent by salinity changes.

**Effect of wind stirring**

An example of short term variability due to weather conditions was observed in the Celtic Sea front in July 1975 when a storm occurred between repeated crossings of one particular section (sections 1 and 2; Fig. 1). The times of these crossings are indicated in Figure 10 (a) where  $\overline{W^3}$  is the wind mixing term in equation (1). The effect of strong wind mixing during the storm depressed the thermocline to  $\sim 30$  m and increased the maximum vertical temperature gradients from 0.3 to 1°C/m. The average increase in heat content of a water column,  $Q$ , for the section, is of the same order as that calculated from the heat balance of Budyko (1974), but there is considerable variation in  $Q$  across the section

after the storm, implying extensive horizontal mixing [Fig. 10 (b)].

The average decrease in  $\overline{V}$  for the section was  $\sim 10 \text{ J.m}^{-3}$  compared with a decrease in  $\overline{V}$  of  $\sim 15 \text{ J.m}^{-3}$  due to the heat input during the six day period if there was no mixing [Fig. 10 (c)].

It is evident then that although the wind mixing due to the storm is significant, it has not destroyed the front to any great extent. This agrees with previous inferences (Simpson, Allen, Morris, 1978) that the wind mixing is of secondary importance compared to the tidal mixing during the summer regime. As the front weakens in the Autumn, any strong wind mixing would then help to destroy the remaining stratification.

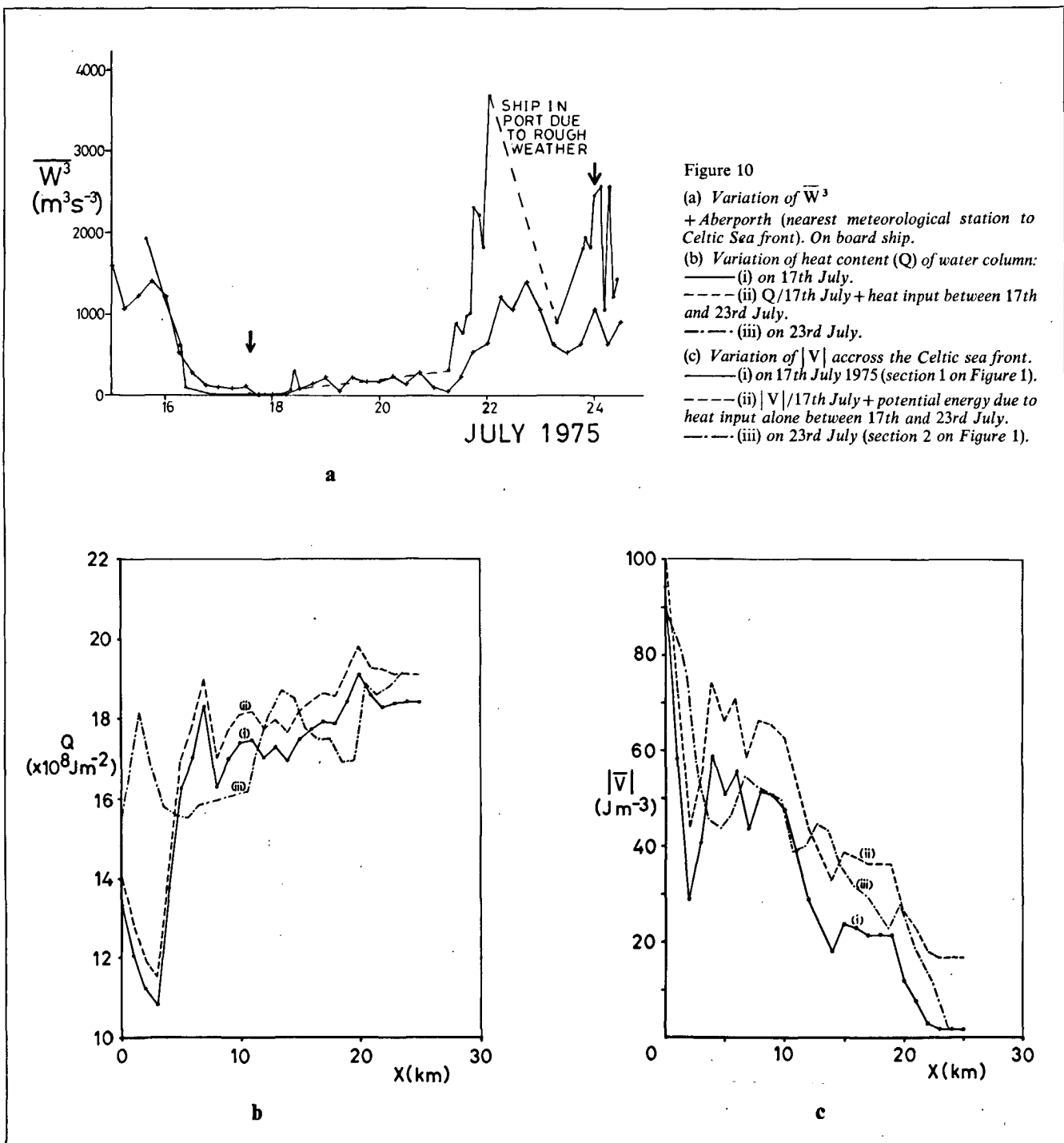


Figure 10  
 (a) Variation of  $\overline{W^3}$  + Aberporth (nearest meteorological station to Celtic Sea front). On board ship.  
 (b) Variation of heat content ( $Q$ ) of water column:  
 — (i) on 17th July.  
 - - - (ii)  $Q$ /17th July + heat input between 17th and 23rd July.  
 - · - · (iii) on 23rd July.  
 (c) Variation of  $|\overline{V}|$  across the Celtic sea front.  
 — (i) on 17th July 1975 (section 1 on Figure 1).  
 - - - (ii)  $|\overline{V}|$ /17th July + potential energy due to heat input alone between 17th and 23rd July.  
 - · - · (iii) on 23rd July (section 2 on Figure 1).



## MIXING EFFICIENCY NEAR A FRONT

Since these shallow sea fronts exist as a result of a balance between solar heat input and tidal mixing, it would seem instructive to investigate variations in the level of mixing along sections perpendicular to the front. Simpson, Hughes and Morris (1977) found that the fraction of tidal energy available for mixing is less than 0.5%. Such estimates are subject to considerable error because of the uncertainty in the size of the drag coefficients and the rate of heat input to the sea surface. Here we use an alternative approach based on calculating the efficiency of mixing relative to its value at the transition point where  $\bar{V} \approx 0$ . We are able to use Batfish CTD data to compare the mixing in the stratified, mixed and transition regions.

The model used here is a one-dimensional model of mixing—we are assuming that all mixing is vertical and ignore any horizontal transfer (which may affect the mixing regime especially in deep water).

The maximum power available in tidal stirring is

$$P_A = \tau u = k \rho \bar{u}^3,$$

where  $k$  is a drag coefficient and  $u$ , the tidal velocity.

The power consumed in working against buoyancy forces— $dW/dt$  may be estimated from changes in potential energy. The mean rate of working between March ( $\bar{V}=0$ ) and July ( $\bar{V}=\bar{V}_j$ ) is

$$\frac{dW}{dt} = \frac{(\bar{V}_j - \bar{V}_m) h}{\Delta t},$$

where  $\bar{V}_m$  is the limiting potential energy density between March and July (time  $\Delta t$ ) in the case of no stirring. The apparent efficiency is thus

$$e = \frac{dW/dt}{P_A} = \frac{(\bar{V}_j - \bar{V}_m) h}{\Delta t k \rho \bar{u}^3} = \frac{(\bar{V}_j - \bar{V}_m)}{\Delta t k \rho} y,$$

where  $y = h/\bar{u}^3$ .

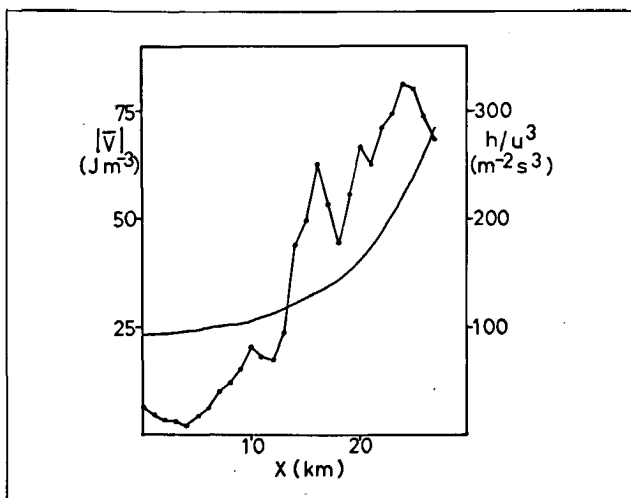


Figure 11  
Variation of  $|\bar{V}|$  and  $h/\bar{u}^3$  across the western Irish sea front on 7th July 1976, section G (marked in Figure 1)

At the front  $\bar{V}_j=0$  and so

$$e_t = \frac{-\bar{V}_m}{\Delta t k \rho} y_t,$$

where  $e_t$  and  $y_t$  are the values of  $e$  and  $y$  at the transition.

An estimate of the relative efficiency of mixing is thus

$$\frac{e}{e_t} = \left(1 - \frac{\bar{V}_j}{\bar{V}_m}\right) \frac{y}{y_t}. \quad (2)$$

The potential energy of the water column,  $\bar{V}_j$  in equation (2), has been calculated from Batfish CTD data;  $\bar{V}_m$ , the limiting potential energy can be calculated from the annual heat balance through the air-sea surface (Budyko, 1974) but in this case it was deduced from most negative  $\bar{V}$  values observed in regions of low tidal streams; values of  $h$  and  $u$  are deduced from a tidal model developed by Pingree and Griffiths (1978).

Figure 11 compares the variation in  $|\bar{V}|$  on crossing the western Irish sea front with that in  $h/\bar{u}^3$ ; the  $|\bar{V}|$  change is much more abrupt.

The efficiency ratio is low in the vertically mixed regime (Fig. 12); this regime is effectively overmixed because there is not enough buoyancy input to absorb all the turbulent kinetic energy available for mixing. The ratio increases linearly with  $y$  because  $\bar{V}_j=0$ , until the transition point of the front where there is a balance between the heat input and the tidal stirring. The efficiency ratio then falls off with increasing stratification, which is suggestive of the form of variation discussed by Linden (1979).

The subsequent rise of  $e/e_t$  with  $y/y_t$  is uncertain because as  $\bar{V}_j \rightarrow \bar{V}_m$  the value of  $\bar{V}_m$ , which is not precisely known, becomes critical in determining the relative efficiency.

The reduced efficiency of mixing with increasing  $y$  corresponds to a lowering of the eddy diffusivity  $A_v$  which occurs in models of vertical mixing like those of James (1977), where  $A_v$  is assumed to depend on

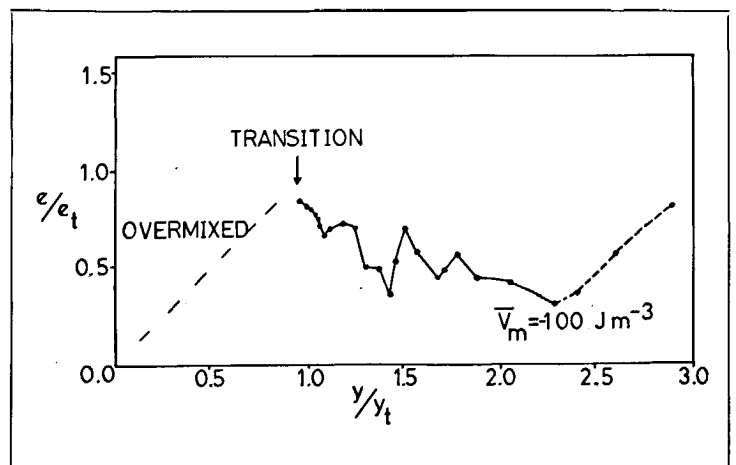


Figure 12  
Efficiency ratio ( $e/e_t$ )  $V h/\bar{u}^3$  ratio  $y/y_t$  for the same section as Figure 11.  $\bar{V}_m$  is the limiting potential energy density which would occur for the March-July heat input in the case of no mixing.

Richardson number. The results presented here lend support to the notion of a feedback process which is implicit in such formulations.

## DISCUSSION

These detailed observations using Batfish CTD indicate several important features of the shelf sea frontal regions. They confirm the existence of complex temperature and density fields with the high resolution data giving evidence of instabilities and internal waves occurring around the thermocline.

The frontal structure appears to deform elastically during a 12 1/2 hour tidal cycle and returns to its original state. This tidal deformation of the front does not induce density instabilities although at low water the isotherms are almost vertical. This suggests the interesting possibility that tidal shear exerts a control on the density structure, in which the mean slope of the isotherms may be determined by the constraint that they should not overturn at any time during the tidal cycle. The development of excessive isotherm slope would result in static instabilities with consequent convective mixing.

In an example studied in July, during the period of maximum intensity of the front, it was found that wind mixing does not destroy the stratification to any great extent but serves to depress the thermocline and intensify the vertical gradients.

Repeated sections at intervals along the front show significant changes in mean isotherm slope, frontal direction, pycnocline intensity and internal wave activity. This along-front variability together with evidence from infra-red satellite imagery (Simpson, Allen, Morris, 1978; Pingree, 1978) point to the inadequacy of 2-dimensional theoretical models in describing these fronts.

The observed variation in the efficiency of mixing near a front is consistent with a positive feedback process, which would mean that, once stratification has been established, it is more difficult to destroy it. Evidence from infra-red satellite imagery suggests that the western Irish sea front and other shelf sea fronts do not adjust significantly to the spring-neap cycle of the tides (Simpson, Bowers, 1979). This would be in accord with the idea that the mixing efficiency is a function of the density stability. Such a dependence is incorporated in the 1-dimensional

model of James (1977) which, in consequence, makes a satisfactory prediction of the non-adjustment to the phase inequality.

## Acknowledgements

We should like to thank Vince Lawford and John Smithers of the Institute of Oceanographic Sciences (Wormley) for operating the Batfish CTD system.

## REFERENCES

- Bowden K. F., Fairbairn L. A., 1952. A determination of the frictional forces in a tidal current, *Proc. Roy. Soc. London, Ser. A*, **214**, 371-392.
- Brown N., 1974. A precision CTD microprofiler. Ocean 74. IEEE International conference on engineering in the ocean environment, IEEE publication 74 CHO 873-0 OCC, Vol. 2, 270-278.
- Bruce R. H., Aiken J., 1975. The undulating oceanographic recorder—A new instrument system for sampling plankton and recording physical variables in the euphotic zone from a ship underway, *Mar. Biol.*, **32**, 85-97.
- Budyko M. I., 1974. *Climate and Life*, Academic Press, 508 p.
- Dessureault J. G., 1976. "Batfish"—a depth controllable towed body for collecting oceanographic data, *Ocean Eng.*, **3**, 99-111.
- James I. D., 1977. A model of the annual cycle of temperature in a frontal region of the Celtic Sea, *Estuarine Coastal Mar. Sci.*, **5**, 339-353.
- James I. D., 1978. A note on the circulation induced by a shallow sea front, *Estuarine Coastal Mar. Sci.*, **7**, 2, 197-202.
- Linden P. F., 1979. Mixing in stratified fluids, *Geophys. Astrophys. Fluid Dyn.*, **13**, 3-23.
- Pingree R. D., 1978. Cyclonic eddies and cross-frontal mixing, *J. mar. biol. Ass. U.K.*, **58**, 955-963.
- Pingree R. D., Griffiths D. K., 1978. Tidal fronts in shelf seas around the British Isles, *J. Geophys. Res.*, **83**, 9, 4615-4622.
- Pingree R. D., Holligan P. M., Head R. N., 1977. Survival of Dinoflagellate blooms in the Western English Channel, *Nature*, **265**, 266-268.
- Savidge G., 1976. A preliminary study of the distribution of chlorophyll 'a' in the vicinity of fronts in the Celtic and Western Irish Sea, *Estuarine Coastal Mar. Sci.*, **4**, 617-625.
- Simpson J. H., 1976. A boundary front in the summer regime of the Celtic Sea, *Estuarine Coastal Mar. Sci.*, **4**, 71-81.
- Simpson J. H., Hunter J. R., 1974. Fronts in the Irish Sea, *Nature*, **250**, 404-406.
- Simpson J. H., Allen C. M., Morris N. C. G., 1978. Fronts on the Continental Shelf, *J. Geophys. Res.*, **83**, 9, 4607-4614.
- Simpson J. H., Edelsten D. J., Edwards A., Morris N.C.G., Tett P. B., 1978. The Islay Front: physical structure and phyto-plankton distribution, *Estuarine Coastal Mar. Sci.*, in press.
- Simpson J. H., Hughes D. G., Morris N. C. G., 1977. The relation of seasonal stratification to tidal mixing on the continental shelf, *Deep-Sea Res.*, Deacon Birthday Volume, *A Voyage of Discovery*, edited by M. Angel, 327-340.
- Simpson J. H., Bowers D., 1979. Shelf sea fronts' adjustment revealed by satellite IR imagery, *Nature*, **280**, 648-650.